

Analysis of Longitudinal Leaky SAW on LiNbO₃/Amorphous Layer/Quartz Structure

LiNbO₃/アモルファス層/水晶構造における縦型リーキーSAWの解析

Shiori Asakawa^{1‡}, Junki Hayashi¹, Masashi Suzuki¹, Shoji Kakio¹, Ami Tezuka², Hiroyuki Kuwae², Hiroaki Yokota³, Toshifumi Yonai³, Kazuhito Kishida³, and Jun Mizuno² (¹Univ. of Yamanashi, ²Waseda Univ., ³The Japan Steel Works, Ltd.)
 浅川 詩織^{1‡}, 林 純貴¹, 鈴木 雅視¹, 垣尾 省司¹, 手塚 彩水², 桑江 博之², 横田 裕章³, 米内 敏文³, 岸田 和人³, 水野 潤² (¹山梨大学, ²早稲田大学, ³日本製鋼所)

1. Introduction

To develop next-generation communication systems, high-performance surface acoustic wave (SAW) devices with high frequency, a large electromechanical coupling factor (K^2), and a large Q factor are required. A structure of different materials bonded together with a longitudinal leaky SAW (LLSAW), advantageous for realizing high frequencies, has been proposed. We previously reported that when a LiNbO₃ (LN) thin plate with a thickness less than the wavelength λ was bonded to a quartz substrate, LLSAW propagation and resonance properties better than those on the single LN substrate were obtained.¹ However, the measured Q factors and temperature coefficients of frequency were different from the theoretical values owing to the nonuniformity of the bonding interface. To improve these values, the strength of the bond between the LN thin plate and the quartz was greatly increased by using amorphous SiO₂ and Al₂O₃ thin films of 50 nm thickness formed by ion beam sputtering as an intermediate layer.² In this study, the propagation and resonance properties of an LLSAW on an amorphous layer between an LN thin plate and a quartz substrate were investigated.

2. Analytical Solution

First, the attenuation and K^2 were calculated for an LLSAW on an amorphous layer inserted between an X-cut 36° Y-propagating LN (X36°Y-LN) thin plate and X-cut 35° Y-propagating quartz (X35°Y-Q) substrate. **Figure 1** shows (a) the attenuation on the metallized surface and (b) K^2 for the LLSAW as a function of the normalized LN thin-plate thickness (h/λ). SiO₂, AlN, and Al₂O₃ were selected as the materials of the amorphous layer. The above-mentioned film thickness h_A was set to 0.01λ . K^2 was determined from the relationship $K^2=2(v_f-v_m)/v_f$, where v_f and v_m are the phase velocity on the free and metallized surface, respectively. The results for the case without the amorphous layer are also shown in these figures.

As shown in Fig. 1(a), the minimum value of

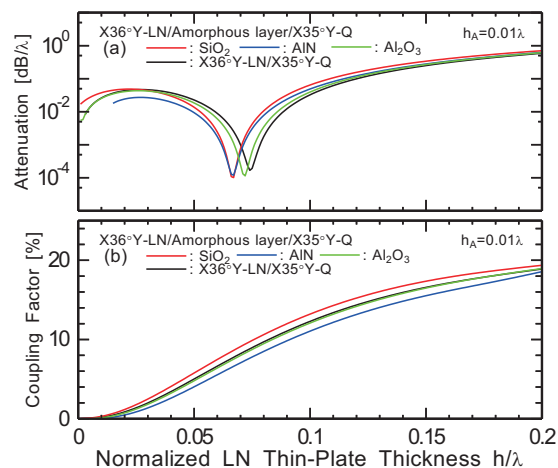


Fig. 1 (a) Attenuation and (b) K^2 as a function of normalized LN thin-plate thickness for LLSAW.

the attenuation on the metallized surface of X36°Y-LN/amorphous layer/X35°Y-Q structure shifted to a smaller thickness of the LN plate. The Al₂O₃ layer was found to have little variation of the minimum attenuation value. The minimum attenuation value was 0.0001 dB/λ at h/λ of 0.072. The value is lower than that in case where no amorphous layer is provided; therefore, the Q factor is expected to be high. Also, as shown in Fig. 1(b), K^2 for the LLSAW increased with increasing h/λ . At h/λ with the minimum attenuation, K^2 for the LLSAW was 9.1%, 7.0%, and 8.0% for SiO₂, AlN, and Al₂O₃, respectively. The results indicate that inserting an amorphous layer increases the bonding strength while maintaining high frequency and a large K^2 . In addition, the improvement of the Q factors can be expected.

3. Finite Element Method Analysis

Using a finite element method (FEM) system, we simulated the resonance properties for X36°Y-LN/amorphous layer/X35°Y-Q. Assuming an infinite periodic single-electrode interdigital transducer (IDT) with wavelength $\lambda=8\ \mu\text{m}$ and an aperture width (W) of 25λ (1,000-Å-thick Al) as the simulated model, the LN plate thickness h and

Al_2O_3 film thickness were set to 0.05λ – 0.07λ and 0.01λ , respectively. The same structure, but in which the mechanical loss Q_m of LN was taken into consideration, was also simulated. **Figure 2** shows the simulation results for these structures with (a) SiO_2 and (b) Al_2O_3 . As shown in Fig. 2(a) and (b), the Q factor when $h/\lambda=0.07$ was found to be 64,000 and 82,000, respectively. By inserting an Al_2O_3 layer, the Q factor was significantly improved compared with that of X36°Y-LN/X35°Y-Q with $h/\lambda=0.08$ having a Q factor of 15,000. When Q_m of 1,000 was assumed, the Q factors were 2,400, 2,500, and 1,900 with inserted SiO_2 , and Al_2O_3 and without an amorphous layer, respectively.

Furthermore, to discuss the low attenuation achieved upon inserting an Al_2O_3 layer in an X36°Y-LN/X35°Y-Q, we examined the particle displacements u_1 , u_2 , and u_3 , which are the main displacement, SH, and SV components of the LLSAW at the resonance frequency (f_r), respectively. **Figure 3** shows the simulated particle displacements u_1 , u_2 , and u_3 for the LLSAW on (a) X36°Y-LN/X35°Y-Q and (b) X36°Y-LN/ Al_2O_3 /X35°Y-Q. As shown in Fig. 3(a), u_1 and u_2 were concentrated on the surface. Also, as shown in Fig. 3(b), u_1 , u_2 , and u_3 were concentrated in the vicinity of the surface. Therefore, it is considered that the attenuation was reduced by the suppression of the leakage of the SV wave mode when the Al_2O_3 layer was inserted. In addition, the increase in the amplitude intensity of the main displacement is also a cause of the high Q factor.

4. Conclusions

In this study, to obtain a low attenuation, the propagation and resonance properties of an LLSAW on an X36°Y-LN/ Al_2O_3 /X35°Y-Q structure were investigated. The attenuation on the metallized surface of the structure was calculated to be 0.0001 dB/ λ at $h/\lambda=0.072$ and was lower than that on an X36°Y-LN/X35°Y-Q structure. Using an FEM system, the inserted Al_2O_3 layer with the X36°Y-LN/X35°Y-Q structure was found to be effective for improving the Q factor of the LLSAW through the surface concentration of the particle displacements. In the future, the X36°Y-LN/ Al_2O_3 /X35°Y-Quartz structure will be investigated experimentally.

Acknowledgments

This work was supported by JSPS Grant-in-Aid for Scientific Research (B) no. 17H03233.

References

1. J. Hayashi *et al.*, Jpn. J. Appl. Phys. **58** (2019) SGGC12.

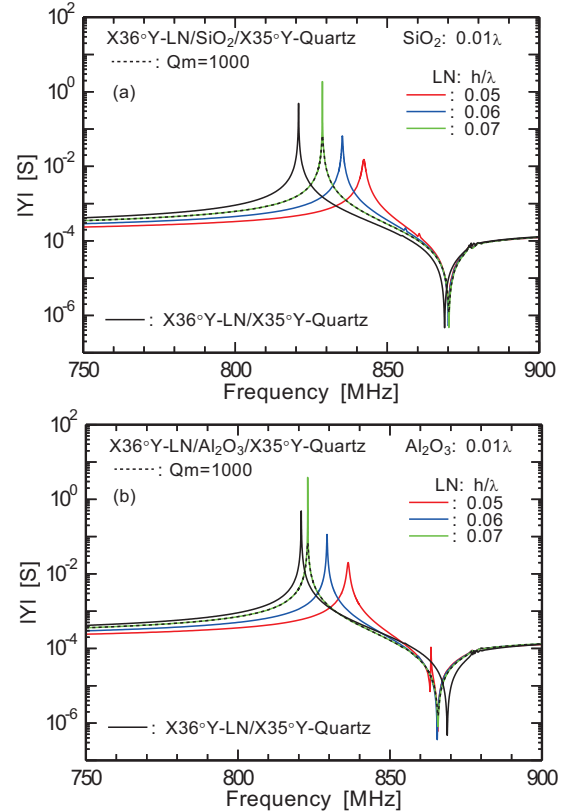


Fig. 2 Simulated resonance properties for LLSAW for (a) SiO_2 and (b) Al_2O_3 .

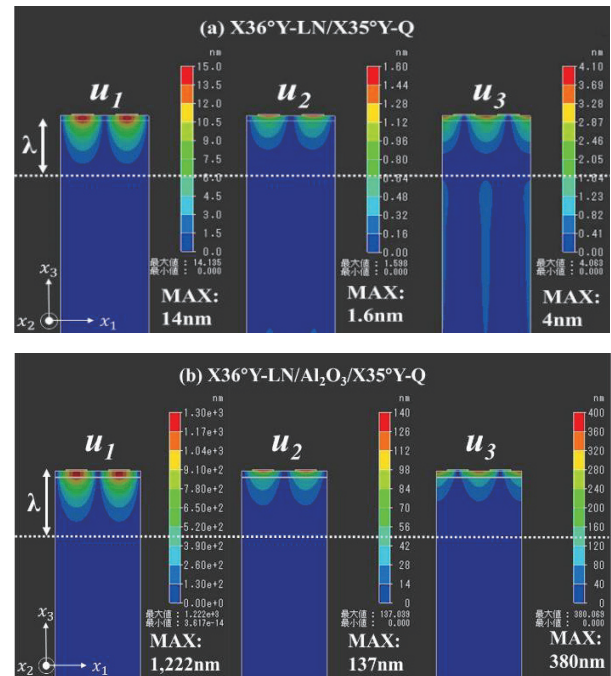


Fig. 3 Simulated particle displacements for LLSAW for (a) X36°Y-LN/X35°Y-Q and (b) X36°Y-LN/ Al_2O_3 /X35°Y-Q.

2. H. Suzaki *et al.*, 24th Symp. Microjoining and Assembly Technology in Electronics, A-2-9, 2018.